Journal of Solid State Chemistry **143,** 285–295 (1999)
Article ID jssc.1998.8110, available online at http://www.idealibrary.com on IDEAL®

Structural Disorder in Solid *p*-Iodotoluene

Heliodoro Serrano-González, Kenneth D.M. Harris,[1] and Simon J. Kitchin

School of Chemistry, University of Birmingham, Edgbaston, Birmingham B15 2TT, United Kingdom

Angel Alvarez-Larena and Eugènia Estop

Unitat de Cristal.lografia i Mineralogia, Universitat Autònoma de Barcelona, 08193 Bellaterra, Spain

Xavier Alcobé

Serveis Cientifico-Tecnics, Universitat de Barcelona, 08028 Barcelona, Spain

Esperanza Tauler and Manuel Labrador

Departament de Cristal.lografia Mineralogia i Dipòsits Minerals, Facultat de Geologia, Universitat de Barcelona, 08028 Barcelona, Spain

and

David C. Apperley

Industrial Research Laboratories, University of Durham, Durham DH1 3LE, United Kingdom

Received August 17, 1998; in revised form November 10, 1998; accepted November 11, 1998

Single crystal X-ray diffraction studies have been carried out on *p*-iodotoluene at two temperatures (293 and 173 K) in order to explore the existence and temperature-dependence of orientational disorder in the crystal structure. In the average crystal structure at each temperature, the molecules are disordered between two orientations. The two orientations define a "head–tail" type of disorder in which the intramolecular $CH_3 \rightarrow I$ vectors are essentially antiparallel and the molecular planes are essentially coplanar. The structures at 293 and 173 K are essentially the same, except that there is a significant difference in the degree of disorder (the fractional occupancy of the minor molecular orientation is 0.17 at 293 K and 0.08 at 173 K). As the same crystal was used for the X-ray diffraction studies at both temperatures, the change in occupancy with temperature suggests that a mechanism exists for the molecular orientation to relax within the crystal. Solid state ^{13}C NMR results are also consistent with (although do not prove) the suggested dynamic interconversion between the two molecular orientations. Several aspects of the disorder in this system are discussed in detail, including an assessment of energetic aspects concerning the different molecular orientations within the crystal.

1. INTRODUCTION

An area of considerable interest within the field of molecular solid state chemistry concerns the concept of miscibility of crystalline phases, and the properties of so-called "molecular alloys." In this regard, molecular miscibility in *para*-disubstituted benzenes (X–C_6H_4–Y, where X and Y represent Cl, Br, I, or CH_3) has been the subject of wide ranging studies, including detailed characterization of the temperature-composition phase diagrams of several binary mixtures of these components (1–3). However, in order to understand the factors that determine the formation of these mixed crystals, it is fundamentally important to understand the structural properties of the pure phases, and here we focus on unsymmetric members within this family (i.e., with $X \neq Y$). The crystal structures of some of the pure phases are already known (at least in specific temperature ranges), including Br–C_6H_4–Cl (4,5), Cl–C_6H_4–I (6,7), Br–C_6H_4–I (8,9), CH_3–C_6H_4–Cl (10), CH_3–C_6H_4–Br (10) and CH_3–C_6H_4–I (11). In the present paper, we report a detailed investigation of the structural properties of one of these materials, *p*-iodotoluene (CH_3–C_6H_4–I). In particular, we focus on the structural disorder in this crystalline solid.

The crystal structure of *p*-iodotoluene at ambient temperature was reported previously (11) to be orthorhombic ($P2_12_12_1$ $(Z = 4)$; $a = 7.46(1)$ Å, $b = 16.50(2)$ Å, $c =$

[1] To whom correspondence should be addressed.

0022-4596/99 $30.00

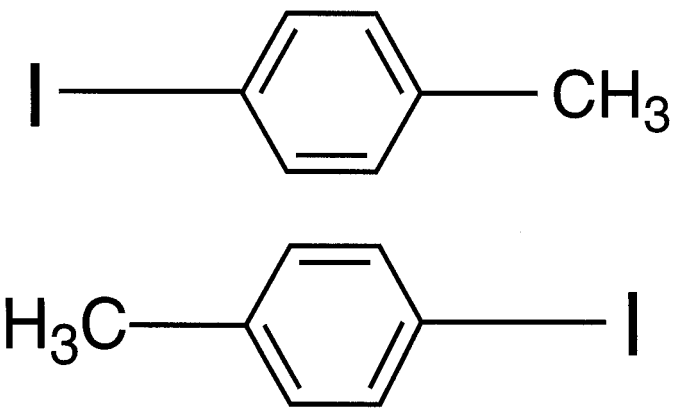

FIG. 1. Schematic illustration showing two different orientations of the *p*-iodotoluene molecule representing head–tail disorder. The molecular planes lie in the same plane, and the molecular axes (defined by the intramolecular $CH_3 \rightarrow I$ vectors) are antiparallel.

6.11(1) Å), with the molecule disordered between two different orientations (described here as head–tail disorder (see Fig. 1)). The occupancies of the two molecular orientations were reported to be 84 and 16% at ambient temperature. If instead there were equal numbers of molecules in each orientation (i.e., occupancies of 50%), the average crystal structure would have an inversion center and the space group would become *Pbca*. The reported partial (16%) disorder for *p*-iodotoluene represents an exception in comparison with other unsymmetrically *para*-disubstituted benzenes, in that Br–C_6H_4–Cl (4, 5), Cl–C_6H_4–I (6, 7), Br–C_6H_4–I (8, 9), CH_3–C_6H_4–Cl (10), and CH_3–C_6H_4–Br (10) all exhibit 50% head–tail disorder at ambient temperature. In this paper, we focus on the temperature dependence of the disorder in *p*-iodotoluene, providing new insights into the nature of the disorder in this solid.

2. EXPERIMENTAL

Single crystals of *p*-iodotoluene were obtained by slow sublimation of a commercial sample (Fluka; purity >99%). A crystal suitable for single crystal X-ray diffraction experiments was selected and fixed inside a capillary (Lindemann) tube using perfluoropolyether. The capillary was sealed to avoid sublimation of the crystal. Single crystal X-ray diffraction experiments were carried out at ambient temperature and at 173 K on an Enraf-Nonius CAD4 diffractometer using graphite monochromated Mo$K\alpha$ radiation. The same crystal was used for the data collections at both temperatures. Accurate lattice parameters were determined by least-squares refinement of the setting angles for 25 automatically centered reflections.

At ambient temperature ((293 ± 2) K), the metric symmetry is orthorhombic, with lattice parameters $a =$ 6.098(1) Å, $b = 7.424(3)$ Å, $c = 16.454(3)$ Å (cell volume = 744.9(4) Å^3). Intensity data were recorded at 293 K in ω-2θ scan mode and comprised the measurement of 5237 reflections ($R_{int} = 0.020$; 1310 independent reflections), of which 3400 were considered as observed based on the criterion $I > 2\sigma(I)$. The data collection was in the range $2.51^\circ \leq \theta \leq 24.99^\circ$, corresponding to $-7 \leq h \leq 7$, $-8 \leq k \leq 8$, and $0 \leq l \leq 19$. The absorption coefficient ($\mu = 4.196$ mm^{-1}) is high, and an empirical absorption correction ($T_{min} = 60$, $T_{max} = 100$) was applied. The Laue group is *mmm*, and systematic absences are consistent with space group $P2_12_12_1$. With four molecules in the unit cell, the density is calculated to be 1.944 g cm^{-3}.

At 173 K, the metric symmetry is orthorhombic, with lattice parameters $a = 6.058(1)$ Å, $b = 7.309(3)$ Å, $c =$ 16.245(3) Å (cell volume = 719.3(3) Å^3). Intensity data were recorded at 173 K in ω-2θ scan mode, and comprised the measurement of 2620 reflections ($R_{int} = 0.012$; 1310 independent reflections) of which 2365 were considered as observed based on the criterion $I > 2\sigma(I)$. The data collection was in the range $2.48^\circ \leq \theta \leq 25.10^\circ$, corresponding to $-7 \leq h \leq 7$, $0 \leq k \leq 8$ and $0 \leq l \leq 19$. The absorption coefficient ($\mu = 4.346$ mm^{-1}) is high, and an empirical absorption correction ($T_{min} = 60$, $T_{max} = 100$) was applied. The Laue group is *mmm*, and systematic absences are consistent with space group $P2_12_12_1$. With four molecules in the unit cell, the density is calculated to be 2.013 g cm^{-3}.

Crystal structure solution was carried out using the direct methods implementation in the program SHELXS-86 (12). Structure refinement calculations were carried out using the programs SHELXL-93 (13) and FULLPROF (14). Full details are given in Sections 3.2 and 3.3.

Powder X-ray diffraction patterns were recorded using Cu$K\alpha_1$ radiation (graphite secondary monochromator) on a Siemens D-500 powder diffractometer operated in Bragg-Brentano θ-2θ mode. Measurements at nonambient temperatures were carried out using a TTK low temperature cell. The same powder sample was used for all measurements. The sample was first cooled to 133 K, and diffractograms were then recorded at several temperatures on heating up to 305 K (the melting temperature of *p*-iodotoluene is 306 K (15)). For each diffractogram, the 2θ range was 9° to 80°, the step size was 0.05°, and the counting time was 10 s per step. Approximately 15 minutes were allowed for the sample to reach thermal equilibrium before recording the data at each temperature.

High-resolution solid state ^{13}C NMR spectra were recorded for a polycrystalline sample of *p*-iodotoluene at several temperatures between 223 and 293 K using a Varian Unity Plus Spectrometer ($B_o = 7.05$ *T*, ^1H frequency 300 MHz). The spectra were recorded using $^1H \rightarrow {}^{13}C$ cross-polarization with flip-back, magic angle sample spinning and high-power ^1H decoupling. The recycle delay was 7 s and the cross-polarization contact time was 1 ms.

3. RESULTS AND DISCUSSION

3.1. Powder X-Ray Diffraction

Powder X-ray diffraction experiments (Fig. 2) were carried out at different temperatures in order to obtain qualitative insights into the variation of the diffraction pattern with temperature. In particular, these experiments allow an assessment of the intensities of those reflections that are present for space group $P2_12_12_1$ but become systematically absent for space group *Pbca*. As discussed above (see also Ref. 16), if the degree of head–tail disorder in *p*-iodotoluene increases with temperature (approaching 50% disorder at sufficiently high temperature), these reflections are expected to decrease in intensity as temperature is increased (approaching zero intensity at sufficiently high temperature). As seen in Fig. 2, the reflections that would become systematically absent in *Pbca* do indeed decrease in intensity as temperature is increased, although they do not become totally absent, even just below the melting temperature (306 K (15)). In particular, the intensity of the peak at $2\theta \approx 13.0^\circ$ (indexed as $\{110\}$ with respect to the transformed cell $a = 16.45$ Å, $b = 7.42$ Å, $c = 6.10$ Å) decreases significantly as temperature is increased. The variation of the relative intensities of peaks in the powder diffraction pattern with temperature may be attributed to a variation of the degree of disorder. To assess this issue more directly and to quantify the degree of disorder, we now discuss our single crystal X-ray diffraction experiments on *p*-iodotoluene at 293 and 173 K.

3.2. Structure Determination at 293 K

3.2.1. Structure solution and preliminary refinement. From the single crystal X-ray diffraction data recorded at 293 K and structure solution by direct methods, all the atoms of one molecule were located. Conventional least-squares refinement (using SHELXL-93) was then carried out, although it was found after a few cycles that the C–CH_3 distance (1.69 Å) had become significantly longer than typical distances (ca. 1.51 Å (17)) for bonds of this type. Furthermore, the isotropic displacement parameter for the methyl carbon atom became particularly low ($U_{iso} = 0.011$ Å^2). These observations are consistent with head-to-tail disorder, with the structure solution presumably having found the molecular orientation of higher occupancy. The problems in refining the carbon atom of the methyl group arise because it is close to the iodine atom of the other molecular orientation (which at this stage was not included in the structural model). Such disorder is consistent with the structure at ambient temperature reported previously (11).

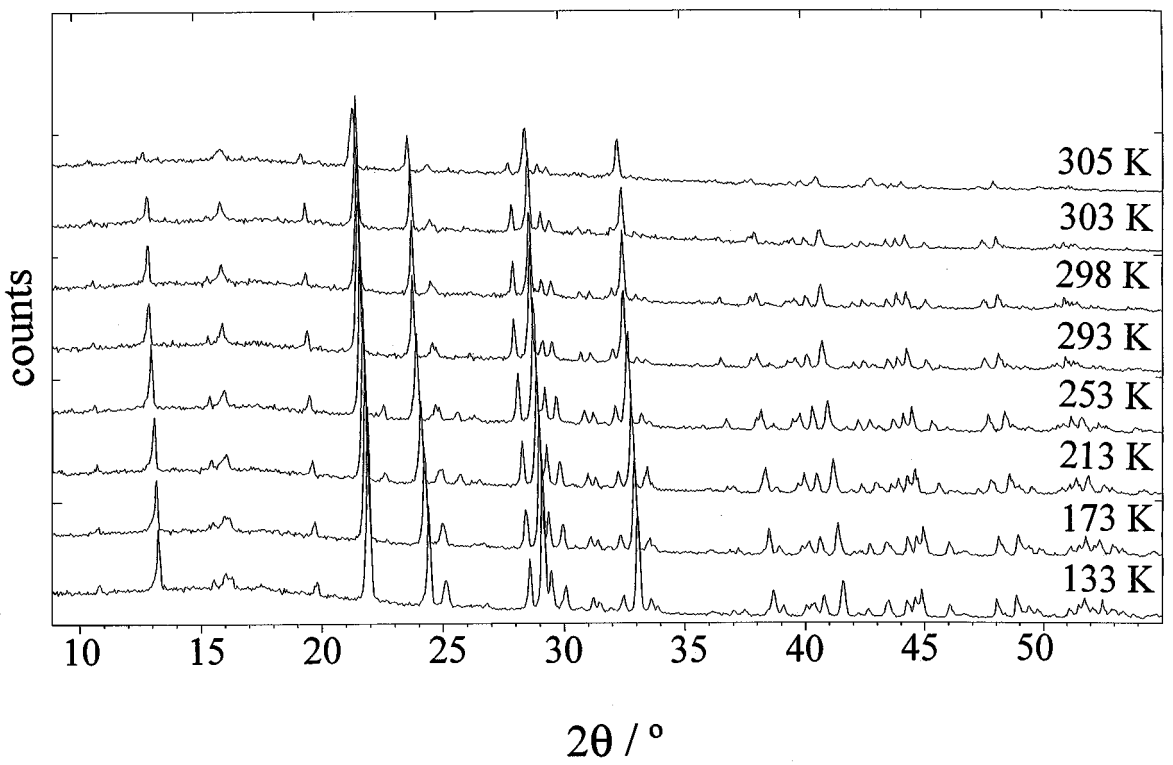

FIG. 2. Powder X-ray diffraction patterns of *p*-iodotoluene recorded (Cu$K\alpha_1$ radiation) as a function of temperature. The extra peaks that appear in the diffractogram at $2\theta \approx 22.7^\circ$ and 25.8° in the temperature range 213–253 K are due to a small amount of ice formation.

To take account of this disorder in the structure refinement calculations, an asymmetric unit comprising two molecules with fractional occupancies must be considered. However, it is important that such refinements are handled in a sensible and rational manner that does not involve simultaneous refinement of parameters that are likely to be highly correlated. These issues are particularly important in the present case as atoms from the two molecular orientations are believed to be almost superimposed on each other (in the average structure). To gain insight into the disorder, we focus on understanding the relative positions and orientations of the molecules in the average structure and the relative amounts (occupancies) of each molecular orientation. Accurate determination of the molecular geometry is not viable for such a disordered system, and indeed if the molecule were treated as completely flexible in the refinement, problems due to correlation of parameters would probably result. For these reasons, refinement strategies involving restriction of the molecular geometry are essential, and we have taken two such approaches. Strategy I is a conventional refinement procedure, but with appropriate restraints and constraints applied to selected parameters during the refinement. Strategy II is a true rigid body refinement, in which parameters describing the intramolecular geometry are not altered during the refinement.

3.2.2. Refinement strategy I. Initially, the molecule located in the structure solution (assigned as the molecular orientation of higher occupancy) was considered, with the aim of locating the second molecular orientation using difference Fourier methods. As discussed above, appropriate restraints and/or constraints on the molecular geometry were introduced to ensure well-behaved refinement. We use "restraint" to mean a soft condition, with the relevant parameter refined subject to an expected error (and thus with the value of the refined parameter effectively limited to a certain range). We use "constraint" to mean an absolute condition, with the relevant parameter fixed at a specific value and not allowed to change in the refinement. These definitions may be extended to the case of relationships imposed between different parameters.

In our initial refinements, the molecule was restrained to be planar, the benzene ring was constrained to be a perfect hexagon with C–C bond distances of 1.39 Å, the C–CH_3 and C–I bond distances were restrained to standard values (17) (1.51 and 2.09 Å, respectively), and the C–I and C–CH_3 vectors were restrained to be collinear (thus maintaining a molecular 2-fold symmetry axis). The occupancy of this molecule was initially fixed at 0.8 (to be refined subsequently), isotropic displacement parameters were fixed at 0.06 $Å^2$ for all carbon atoms, and anisotropic displacement parameters were refined for the iodine atom. The difference Fourier map for this structural model allowed the iodine atom and four carbon atoms of the second molecular orientation to be located. From the positions of these atoms, the complete benzene ring of this molecule could be constructed.

In all subsequent refinement calculations, both molecular orientations were included in the structural model and the geometries of both molecules were constrained/restrained as described above. In the initial refinements, the occupancies of the two molecular orientations were fixed at 0.8 and 0.2. For the high-occupancy molecule, isotropic displacement parameters were refined independently for all carbon atoms of the benzene ring, the isotropic displacement parameter for the methyl carbon atom was fixed at 0.06 $Å^2$, and anisotropic displacement parameters were refined for the iodine atom. For the low-occupancy molecule, isotropic displacement parameters were fixed at 0.06 $Å^2$ for all carbon atoms and anisotropic displacement parameters were refined for the iodine atom. With this refinement strategy, difference Fourier synthesis located the methyl carbon atom of the low-occupancy molecule. This approach led to well-behaved refinement for both molecules.

In the next stage, the occupancies of the two molecular orientations were refined, with the sum of the occupancies constrained to equal unity. Anisotropic displacement parameters were refined for all atoms of the high-occupancy molecule and isotropic displacement parameters were refined for all atoms of the low-occupancy molecule (common values of isotropic displacement parameters were not imposed). In subsequent attempts to introduce anisotropic displacement parameters for the low-occupancy molecule, high correlations involving displacement parameters and positions for certain atoms of the two molecular orientations were found (particularly for atoms that are essentially superimposed in the average structure). For this reason, in our refinements with anisotropic displacement parameters for both the high-occupancy and low-occupancy molecules, the parameters for neighboring (essentially superimposed) atoms of the two molecular orientations were constrained to be the same (and the values allowed to refine). At this stage, hydrogen atoms were placed in calculated positions using a riding model.

In the last stage of refinement, the constraint that the benzene ring is a regular hexagon was relaxed for the high-occupancy molecule (although the 2-fold axis of the *p*-iodotoluene molecule was still imposed). The constraint of hexagonal geometry was still imposed for the benzene ring of the low-occupancy molecule (attempts to relax this constraint led to unreasonable distortions). The C–I bond distances for both molecular orientations were restrained to be equal and the value allowed to refine, and the C–CH_3 bond distances were restrained to the standard value 1.51 Å (17) (attempts to restrain the C–CH_3 bond distances to be equal for the two molecular orientations while allowing the value to refine led to an unacceptably low value of 1.46 Å).

TABLE 1
Final Refined Coordinates, Occupancies, and Equivalent Isotropic Displacement Parameters for the Crystal Structure of *p*-Iodotoluene at 293 K

Atom	*x/a*	*y/b*	*z/c*	Occupancy	U_{eq}/Å^2
		Major orientation			
I(11)	− 0.02676(9)	− 0.21159(9)	0.92066(3)	0.830(2)	0.092(2)
C(11)	0.1446(8)	− 0.2380(4)	0.8124(4)	0.830(2)	0.060(2)
C(12)	0.0523(10)	− 0.1780(8)	0.7409(3)	0.830(2)	0.062(2)
C(13)	0.1667(11)	− 0.1962(10)	0.6693(4)	0.830(2)	0.073(2)
C(14)	0.3720(10)	− 0.2736(9)	0.6674(4)	0.830(2)	0.076(2)
C(15)	0.4589(12)	− 0.3316(10)	0.7403(4)	0.830(2)	0.076(2)
C(16)	0.3478(9)	− 0.3131(9)	0.8122(4)	0.830(2)	0.071(2)
C(17)	0.4970(19)	− 0.2920(13)	0.5893(6)	0.830(2)	0.095(1)
		Minor orientation			
I(21)	0.5248(7)	− 0.2990(5)	0.5789(2)	0.170(2)	0.095(1)
C(21)	0.377(2)	− 0.2735(17)	0.6903(5)	0.170(2)	0.076(2)
C(22)	0.486(3)	− 0.331(4)	0.7598(6)	0.170(2)	0.076(2)
C(23)	0.387(4)	− 0.314(5)	0.8354(6)	0.170(2)	0.071(2)
C(24)	0.178(4)	− 0.240(4)	0.8416(7)	0.170(2)	0.060(2)
C(25)	0.069(3)	− 0.182(5)	0.7721(9)	0.170(2)	0.062(2)
C(26)	0.168(3)	− 0.199(4)	0.6964(7)	0.170(2)	0.073(2)
C(27)	0.073(5)	− 0.222(5)	0.9239(10)	0.170(2)	0.092(2)

Note. Refinement was carried out on F^2 for reflections with $I > 2\sigma(I)$, with 86 parameters and 28 restraints. The final agreement factors were $R(F) = 0.032$ and $R_w(F^2) = 0.083$, with weighting scheme $w = 1/[\sigma^2(F_o^2) + (0.0599\ P)^2]$ and $P = [2F_c^2 + \max(F_o^2, 0)]/3$. The largest positive and negative features in the difference Fourier map were 0.42 and − 0.21 eÅ^{-3}. The equivalent isotropic displacement parameter U_{eq} is defined as one third of the trace of the orthogonalized U_{ij} tensor. The two disordered molecular orientations at each site in the average crystal structure are shown in Fig. 5.

The final refined occupancies for the two molecular orientations are 0.830(2) and 0.170(2), and the final refined coordinates and equivalent isotropic displacement parameters are shown in Table 1. The structure is described in detail in Section 4. The largest peak in the final difference Fourier map was 0.42 eÅ^{-3}, positioned near the iodine atom of the high-occupancy molecule.

3.2.3. Refinement strategy II. In this approach, the low-occupancy and high-occupancy molecules were handled as rigid fragments with idealized geometry taken as a planar molecule with regular hexagonal benzene ring and bond distances d[C(ring)–C(ring)] = 1.39 Å, d[C–CH$_3$] = 1.51 Å, d[C–I] = 2.09 Å, d[C(ring)–H] = 0.93 Å, d[C(methyl)–H] = 0.96 Å. The method used for rigid body refinement neglects the effects of internal vibrations and assumes that the displacement parameters for all atoms depend solely on the rigid body motion. Thus, instead of refining the fractional coordinates for each atom, only three coordinates and three angles are refined for the whole rigid body. With regard to displacement parameters, the components of the translation tensor (T; 3×3, symmetric), the libration tensor (L; 3×3, symmetric), and the tensor (S; 3×3) that accounts for correlation of libration and translation are refined. Anisotropic displacement parameters for individual atoms may then be derived from the T, L and S tensors (18). These rigid body refinement calculations were carried out using the program FULLPROF (14).

The same rigid geometry was used for both molecular orientations, and the initial positions of these molecules were derived from the structure obtained from Strategy I. Different refinement calculations carried out using different initial occupancies for the two molecular orientations all converged to the same final occupancies. For stable refinement, it was necessary to constrain the T, L, and S tensors to be the same for the two molecular orientations. With this approach, the number of refined parameters is 33 (in comparison with 86 for Strategy I).

The final refined occupancies for the two molecular orientations are 0.8359(8) and 0.1641(8), with final agreement factor $R(F) = 0.069$ $[R(F) = \sum|F_{obs} - F_{calc}|/|F_{obs}|]$. As the components of the T, L, and S tensors were constrained to have the same values for the two molecular orientations, it is not appropriate to analyze in detail the values of these parameters. Nevertheless, we note that the values of the U_{ij} parameters derived from the T, L, and S tensors are physically reasonable.

3.2.4. Assessment of techniques. Here we focus on the method for handling the disorder in the structure. A more detailed description of the structure itself is given in Section 4. As discussed in Section 3.2.1, careful consideration is required in developing and applying sensible strategies for refinement of disordered molecular crystal structures, and in this regard we believe that both Strategies I and II are valid approaches for investigating the structural properties of *p*-iodotoluene. Thus, while Strategy II adopts a classical rigid body refinement, Strategy I allows some relaxation of the molecular geometry subject to appropriate restraints/constraints. Both strategies lead to essentially the same crystal structure, with essentially the same refined occupancies of the two molecular orientations. The refined occupancy of the minor molecular orientation is 0.170(2) from Strategy I and 0.1641(8) from Strategy II (average 0.17). We estimate that a realistic standard deviation in the occupancy is not less than 0.01 (the actual estimated standard deviation in the refined occupancies is significantly lower).

At ambient temperature, the refined occupancies determined here are similar to those reported previously (11) (0.16 for the low-occupancy molecule). The crystal structure reported here is more accurate and precise than that reported previously, with more independent reflections measured (1310 versus 819 in Ref. 11) and probably greater reliability in the measurement. In Ref. 11, the low-occupancy molecule was refined as a rigid unit with idealized

geometry, an isotropic displacement parameter was refined for the iodine atom, a common isotropic displacement parameter was refined for the carbon atoms, and the occupancies were established by trial-and-error. Despite the different approaches and quality of data used, the crystal structure at ambient temperature reported in Ref. 11 is essentially identical to that determined here, with all corresponding structural parameters within 3σ of each other.

3.3. Structure Determination at 173 K

Structure determination using the data recorded at 173 K involved both strategies discussed above. For Strategy I, the crystal structure determined at 293 K was used as the starting model for structure refinement calculations. In the first stage, both the high-occupancy and low-occupancy molecules were restrained to be planar with regular hexagonal geometry of the benzene ring, the C–CH_3 and C–I bond distances were restrained and the positions of the iodine atom and carbon atom of the methyl group were restrained to preserve the molecular 2-fold symmetry axis. The displacement parameters for neighboring atoms of the two molecular orientations were constrained to be the same (for the reasons discussed above). In the last stage of refinement, the procedure reported above for 293 K was followed, but with the C–CH_3 distance restrained to a common value (which was subjected to unrestrained refinement) for the two molecular orientations. The final refined occupancies are 0.917(2) for the high-occupancy molecule and 0.083(2) for the low-occupancy molecule. The final refined coordinates and equivalent isotropic displacement parameters are shown in Table 2.

Strategy II (following the same procedure described above for 293 K) led to final refined occupancies of 0.9255(6) and 0.0745(6) for the two molecular orientations. The final $R(F)$ was 0.038. The average occupancy over both refinement strategies is 0.08, with a realistic standard deviation of about 0.01.

TABLE 2
Final Refined Coordinates, Occupancies, and Equivalent Isotropic Displacement Parameters for the Crystal Structure of *p*-iodotoluene at 173 K

Atom	x/a	y/b	z/c	Occupancy	$U_{eq}/Å^2$
			Major orientation		
I(11)	−0.03653(6)	−0.20927(5)	0.92193(2)	0.917(2)	0.047(1)
C(11)	0.1441(7)	−0.2382(3)	0.8127(3)	0.917(2)	0.034(1)
C(12)	0.0532(8)	−0.1794(5)	0.7394(2)	0.917(2)	0.037(1)
C(13)	0.1726(8)	−0.1995(7)	0.6676(3)	0.917(2)	0.040(1)
C(14)	0.3816(7)	−0.2770(6)	0.6670(3)	0.917(2)	0.040(1)
C(15)	0.4686(9)	−0.3341(6)	0.7422(3)	0.917(2)	0.041(1)
C(16)	0.3520(7)	−0.3142(6)	0.8148(3)	0.917(2)	0.037(1)
C(17)	0.512(2)	−0.2964(10)	0.5888(9)	0.917(2)	0.052(2)
			Minor orientation		
I(21)	0.5301(15)	−0.3019(9)	0.5777(7)	0.083(2)	0.052(2)
C(21)	0.369(3)	−0.262(2)	0.6895(9)	0.083(2)	0.040(1)
C(22)	0.472(5)	−0.312(5)	0.7626(8)	0.083(2)	0.041(1)
C(23)	0.365(7)	−0.285(6)	0.8373(9)	0.083(2)	0.037(1)
C(24)	0.155(6)	−0.209(5)	0.8388(13)	0.083(2)	0.034(1)
C(25)	0.052(5)	−0.159(7)	0.7657(16)	0.083(2)	0.037(1)
C(26)	0.159(4)	−0.186(6)	0.6910(13)	0.083(2)	0.040(1)
C(27)	0.038(8)	−0.180(7)	0.920(2)	0.083(2)	0.047(1)

Note. Refinement was carried out on F^2 for reflections with $I > 2(I)$, with 86 parameters and 27 restraints. The final agreement factors were $R(F) = 0.021$ and $R_w(F^2) = 0.054$, with weighting scheme $w = 1/[\sigma^2(F_o^2) + (0.0350\,P)^2]$ and $P = [2F_o^2 + \max(F_o^2, 0)]/3$. The largest positive and negative features in the difference Fourier map were 0.60 and -0.29 e$Å^{-3}$.

3.4. Solid State NMR

To probe the local structural properties of solid *p*-iodotoluene, we have recorded high-resolution solid state ^{13}C NMR spectra as a function of temperature. The orientational disorder of the molecules in the average crystal structure discussed above should give rise to a distribution of local environments for each type of ^{13}C nucleus in the molecule. If the disorder is static, high-resolution solid state ^{13}C NMR should be able to reveal a distribution of local environments, provided the differences in isotropic chemical shifts for the different environments are significant in comparison with the intrinsic ^{13}C NMR linewidths for each environment. In this regard, the signal for the methyl carbon should be particularly informative, as its linewidth is expected to be narrower than that for the other carbons in the *p*-iodotoluene molecule. Furthermore, it is clear from the structure (see Section 4) that head–tail disorder should correspond to a significant difference in the local environment around the methyl group. Thus, if all molecules were in the major orientation, there would be no $CH_3 \cdots I$ close contacts within a layer, whereas such close contacts are introduced when a molecule is reoriented into the minor orientation. If the disorder becomes dynamic at sufficiently high temperature, the high-resolution solid state ^{13}C NMR spectrum may be expected to exhibit well-defined coalescence phenomena on passing from sufficiently low temperature (dynamics slow with respect to the ^{13}C NMR timescale (i.e., essentially static disorder)) to sufficiently high temperature (dynamics rapid with respect to the ^{13}C NMR timescale).

A representative high-resolution solid state ^{13}C NMR spectrum for *p*-iodotoluene is shown in Fig. 3. At all temperatures studied, only one resolved peak is observed for the methyl carbon. This peak was fitted at each temperature, and in all cases a good fit was obtained using a single line of mixed Gaussian/Lorentzian character (ca. 50% Gaussian and 50% Lorentzian). There was no evidence for asymmetry in the lineshape at any temperature (a distribution of local environments may give rise to peak asymmetry), and no

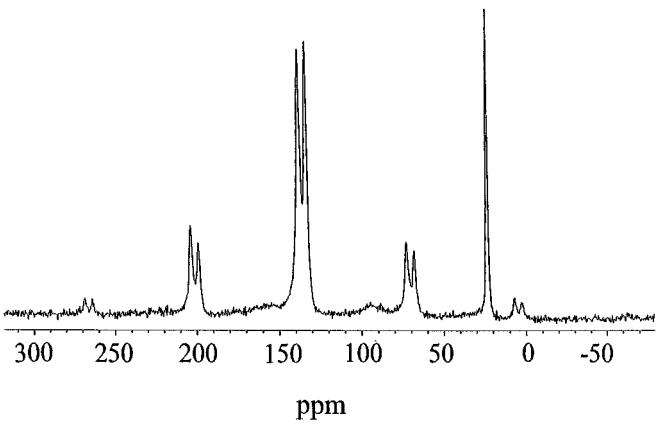

FIG. 3. High-resolution solid state ^{13}C NMR spectrum recorded for *p*-iodotoluene at 223 K. The isotropic peak for the methyl carbon is at 23.0 ppm.

significant changes in the position, linewidth or lineshape of the single line were evident in the temperature range investigated. Thus, on cooling the sample, the single line does not broaden and evolve into two or more lines (de-coalescence) and does not become asymmetric, either of which would signify a distribution of local environments and entry into the temperature regime representing static disorder. The observation of a single symmetric line at all temperatures investigated is consistent with a dynamic interconversion between the major and minor molecular orientations, with the rate of interconversion rapid with respect to the ^{13}C NMR timescale. However, from the ^{13}C NMR data alone, we also cannot rule out the possibility that the system has static disorder at all temperatures investigated, under the (unexpected) circumstances that the isotropic chemical shifts for the methyl carbon in all local environments within the disordered crystal are accidentally indistinguishable.

4. DISCUSSION OF STRUCTURAL PROPERTIES

The crystal structures at 293 and 173 K are essentially the same, and differ only in terms of the overall occupancies of the major and minor molecular orientations. As shown in Fig. 4, the molecules are arranged in "layers" perpendicular to the *b*-axis. The layers at $y \approx 0.25$ and $y \approx 0.75$ are related by the 2_1 screw axis parallel to the *b*-axis (located at the (x, z) positions $(0, \frac{1}{4})$ and $(0, \frac{3}{4})$). The structure of a layer comprising only molecules in the high-occupancy orientation (see Fig. 4) shows clearly that the molecules are arranged in rows

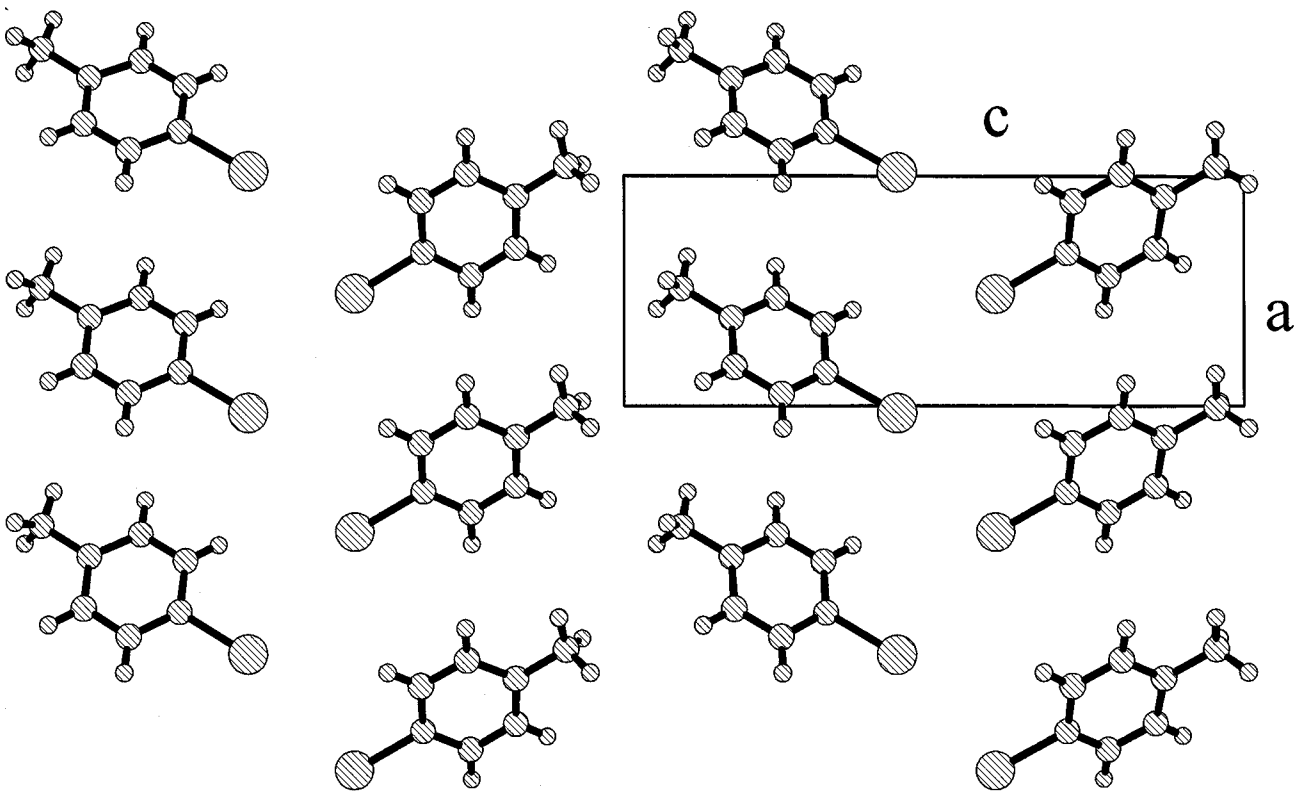

FIG. 4. Crystal structure of *p*-iodotoluene determined at 293 K, viewed here along the *b*-axis and showing only the molecules in the high-occupancy orientation. In the true average crystal structure, each molecular site contains two disordered molecular orientations, as shown in Fig. 5.

parallel to the *a*-axis (vertical in Fig. 4). One "interface" between adjacent rows involves only the iodine atoms and the other "interface" between adjacent rows involves only the methyl groups. The operation of the 2_1 screw axes parallel to the *b*-axis are such that molecules in a given layer are not directly stacked on top of molecules in the adjacent layers.

It is not surprising that head–tail disorder can exist in such structures, as the volume and shape of the space taken up by the two molecular orientations are very similar. The two molecular orientations in a given site are shown in Fig. 5, demonstrating that the intramolecular $CH_3 \rightarrow I$ vectors are essentially collinear (antiparallel) and that the molecular planes are essentially parallel. The distance between the centroids of the benzene rings in the two molecular orientations is 0.45 Å at 293 K and 0.42 Å at 173 K, and the average distance between pairs of related atoms in the two molecular orientations is 0.44 Å at 293 K and 0.41 Å at 173 K. The normals to the planes of the high-occupancy and low-occupancy molecules form an angle of 2.2° at 293 K and 3.4° at 173 K, and the angle between the molecular axes of the high-occupancy and low-occupancy molecules is 4.2° at 293 K and 2.1° at 173 K.

In principle, the disorder in the average crystal structure may be compatible with a variety of local structural situations (e.g., at any instant in time), representing intermediate situations between the following extreme situations.

(1) The crystal comprises domains in which all molecules have the major orientation (defined by the high-occupancy molecule in the average structure) and domains in which all molecules have the minor orientation (defined by the low-occupancy molecule in the average structure).

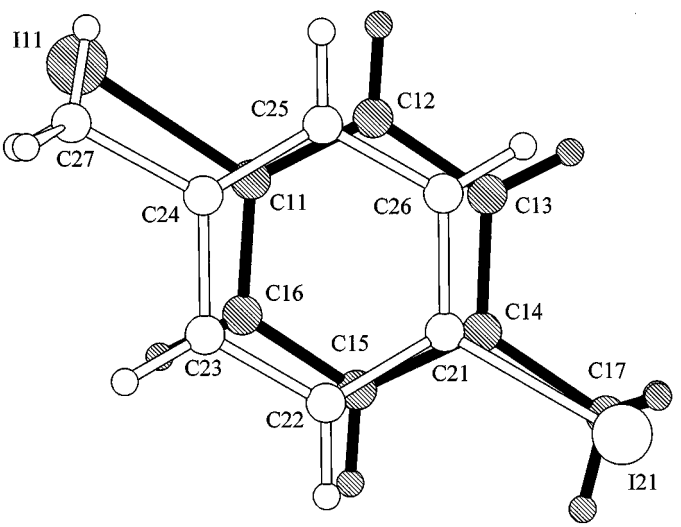

FIG. 5. The two disordered molecular orientations at each site in the average crystal structure of *p*-iodotoluene at 293 K. The atom labeling is the same as that used in Table 1.

(2) The crystal comprises molecules with the major and minor orientations distributed throughout the crystal, with the orientation adopted by the molecule in a given site determined purely on a statistical basis (reflecting the different occupancies for the two molecular orientations in the average structure).

For situation (1), the crystal comprises locally ordered domains, most of which contain only molecules in the major orientation, but some of which contain only molecules in the minor orientation; the relative amounts of these different types of domain give rise to the observed occupancies of the different molecular orientations in the average structure. For situation (2), the crystal comprises a homogeneous domain in which the probability that a molecule in a given site adopts a particular orientation is the same for each site in the crystal and is in principle uncorrelated with the orientations of the neighboring molecules; the relative probabilities of a molecule adopting the major or minor molecular orientation in each site in the crystal determines the observed occupancies in the average structure. Clearly a continuous range of intermediate situations exists between (1) and (2), depending on the extent to which a molecule in the minor orientation (essentially a "defect" in the crystal) influences its neighbors to also adopt the minor orientation. Thus, in situation (1) the orientations of a molecule and its neighbors in a given domain are completely correlated, whereas for situation (2) the orientations of a molecule and its neighbors are completely uncorrelated.

It is possible that one or other of these extremes may give rise to local structural features (e.g., intermolecular contacts) that are implausible, and to assess this issue the intermolecular distances have been considered in detail (using the structure determined at 173 K). The following local structural types have been considered:

(a) a domain in which all molecules have the major orientation (see Fig. 4);

(b) a domain in which all molecules have the minor orientation (see Fig. 6);

(c) a domain in which all molecules have the major orientation but one (central) molecule has the minor orientation.

For situation (1), the crystal must comprise local regions of type (a) and local regions of type (b). Type (c), on the other hand, represents one of the many possible local structural descriptions that may exist for situation (2).

The shortest distances between atoms in neighboring molecules in structural types (a)–(c) are reported in Table 3. There are no obviously unfavorable intermolecular contacts in any of these cases, and none of these local structural descriptions can be rejected on this basis. For (a) and (b), iodine atoms within a layer are at the lower end of the range commonly found (19) for intermolecular I···I interactions and are somewhat shorter than those observed (20) for

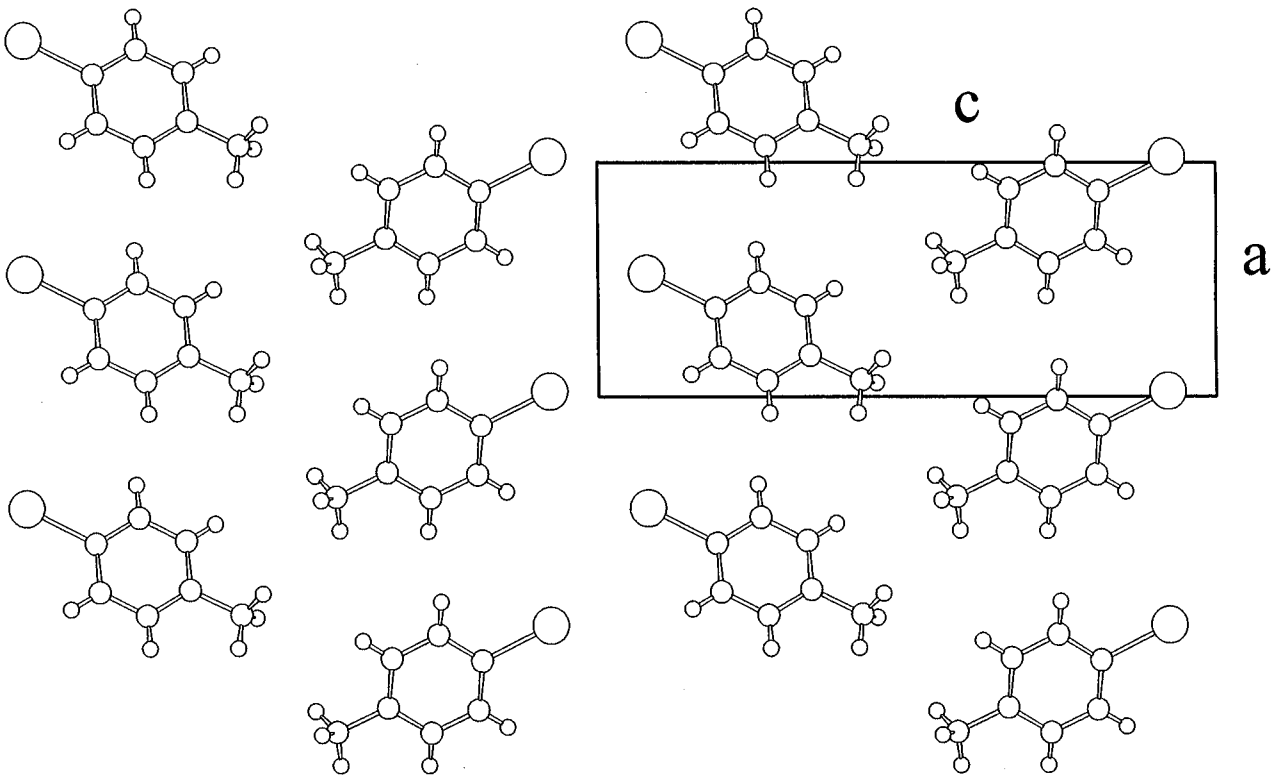

FIG. 6. Representation of an ordered domain of the crystal structure of *p*-iodotoluene containing only molecules in the low-occupancy orientation. The structure is viewed here along the *b*-axis and has been constructed using data for the low-occupancy molecular orientation in the structure determined at 293 K.

p-diiodobenzene (α phase, 4.12(2) Å; β phase, 4.13(2) Å and 4.18(2) Å). For the central molecule in type (c), there are no short I···I distances within the layers, and the shortest I···I distances exist between adjacent layers.

To explore these issues further, the energy for each of the structural types (a)–(c) has been calculated using the program GULP (21) together with atom–atom potentials from Table 3.10 (p. 117) of Ref. 22. These calculations used the unit cell parameters and atomic coordinates of the crystal structure determined at 173 K. No geometry relaxation was carried out and a cut-off radius of 15 Å was used. The domain of the major orientation (type (a)) and the domain of the minor orientation (type (b)) were constructed from the crystal structure determined at 173 K. Periodic boundary conditions were applied in both cases. For the domain (type (c)) comprising a central molecule in the minor orientation with all other molecules in the major orientation, a $3 \times 3 \times 3$ supercell of the crystallographic unit cell was used as the simulation cell, with periodic boundary conditions applied. In this supercell, the molecule in the minor orientation is completely surrounded by molecules in the major orientation and can therefore be regarded as a dilute defect. In this case, the energy has been normalized to a cell 27 times smaller, corresponding to the size of cell used for types (a) and (b). We note that our calculations did not involve energy minimization—i.e., no structural relaxation was allowed. The results are reported in Table 3.

First, we note that the energy of type (a) is lower than the energy of type (b) and provides some justification for the observed preference for the molecular orientation adopted in type (a). Nevertheless, the differences in energy between (a), (b), and (c) are comparatively small, and on this basis none of these structural types can be rejected. The difference in energy between (a) and (c) represents the energy associated with an isolated "defect" molecule adopting the minor orientation within a domain of the major orientation. This defect energy is small, from which we may conclude that no substantial energetic penalty is associated with accommodating a molecule in the minor orientation within a domain of the major orientation. We recall that our calculations did not consider structural relaxation, and an even smaller defect energy may be expected if relaxation of the structure around this defect had been allowed. In summary, our calculations are completely consistent with disorder of the molecular orientation in the crystal structure of *p*-iodotoluene. We next assess whether this disorder is dynamic or static.

TABLE 3
The Shortest Intermolecular Distances for the Three Local Structural Types Discussed in the Text

	Type (a)	Type (b)	Type (c)
C(ring) ⋯C(ring)	3.72 Å	3.69 Å	3.67 Å
C(methyl) ⋯C(methyl)	4.24 Å	4.10 Å	3.91 Å *
I ⋯I	4.00 Å	4.01 Å	4.22 Å *
C(ring) ⋯C(methyl)	3.94 Å *	4.08 Å	α 3.85 Å *
			β 4.02 Å *
C(ring) ⋯I	3.95 Å *	3.79 Å *	α 3.91 Å
			β 4.03 Å *
C(methyl) ⋯I	4.17 Å *	3.80 *	α 3.71 Å
			β 4.04 Å
Energy/kJ (mol cells)$^{-1}$	− 254.54	− 247.79	− 254.47

Note. Distances between molecules in adjacent layers are labelled by an asterisk (*); all other distances are between molecules in the same layer. For type (c), all distances shown are between the central molecule in the minor orientation and its neighbouring molecules. For type (c), when the atom types are not the same (e.g., C(methyl) ⋯I), two distances labelled α and β are given. Label α refers to the case in which the first atom specified (i.e., C(methyl)) is on the central molecule; label β refers to the case in which the second atom specified (i.e., I) is on the central molecule. The calculated energy (as discussed in the text) for each of the three structure types is also given.

As discussed above, our single crystal X-ray diffraction experiments indicate that the degree of disorder changes with temperature, with the occupancy of the minor molecular orientation increasing from 0.08 at 173 K to 0.17 at 293 K, although no other structural changes are evident in this temperature range. Importantly, we emphasize that the same single crystal was used for data collection at both temperatures. If the degree of disorder in a given crystal can change in response to an external stimulus, such as temperature, it is clear that a mechanism must exist for relaxation of the molecular orientation in the crystal. Thus, the temperature dependence of the degree of disorder, observed from our X-ray diffraction analysis, suggests that the disorder is (at least partly) dynamic in character and presumably involves head–tail reorientation of the *p*-iodotoluene molecules. As discussed in Section 3.4, our variable-temperature solid state ^{13}C NMR results suggest that all methyl carbon atoms experience the same local environment when averaged over the timescale of the ^{13}C NMR technique, and this observation is consistent with dynamic interconversion between the two molecular orientations. However, this observation does not prove definitively that a dynamic molecular reorientation process occurs (the single line observed in the ^{13}C NMR spectrum at all temperatures studied would also be consistent with static disorder of the methyl group between sites for which the isotropic chemical shifts are accidentally indistinguishable).

Finally, we note that a detailed study (15) of the thermal properties of *p*-iodotoluene has provided evidence that a glass transition occurs at 250 K, and it has been suggested that this transition is associated with rotational dynamics of the methyl group. Our structural studies reported here shed no further light on the nature of this transition. Detailed structural and spectroscopic studies in the close vicinity of the transition temperature are required to establish more insights into this issue.

In summary, the results reported here demonstrate that there is orientational disorder of the molecules in the crystal structure of *p*-iodotoluene and that this disorder exhibits an interesting temperature dependence. Our results suggest that this disorder may be dynamic. To investigate more directly the existence and nature of molecular dynamics in this system, we are currently extending our present studies using a range of other solid state NMR techniques. Weak diffuse scattering that we have observed in single crystal X-ray diffraction photographs for *p*-iodotoluene is also being studied as a further source of information on the structural disorder in this system.

ACKNOWLEDGMENTS

We are grateful to the University of Birmingham for financial support (studentship to HSG), to the EPSRC Solid State NMR Service for providing facilities for solid state NMR experiments, and to Professor Robin Harris for helpful discussions.

REFERENCES

1. Y. Haget, J. R. Housty, A. Maiga, L. Bonpunt, N. B. Chanh, M. A. Cuevas, and E. Estop, *J. Chim. Phys.* **81,** 197 (1984).
2. L. Bonpunt, R. Courchinoux, Y. Haget, E. Estop, T. Calvet, M. A. Cuevas-Diarte, and M. Labrador, *J. Appl. Crystallogr.* **24,** 164 (1991).
3. T. Calvet, M. A. Cuevas-Diarte, E. Tauler, M. Labrador, Y. Haget, and H. A. J. Oonk, *J. Chim. Phys.* **92,** 2038 (1995).
4. S. B. Hendricks, L. R. Maxwell, V. L. Mosley, and M. E. Jefferson, *J. Chem. Phys.* **1,** 549 (1933).
5. A. Klug, *Nature* **160,** 570 (1947).
6. D. Britton, *Acta Crystallogr. B* **32,** 976 (1976).
7. X. Alcobé, E. Estop, M. A. Cuevas-Diarte, M. Labrador, T. Calvet, and E. Tauler, *J. Appl. Crystallogr.* **20,** 48 (1987).
8. P. N. Prasad and E. D. Stevens, *J. Chem. Phys.* **66,** 862 (1977).
9. M. T. Calvet, X. Alcobé, E. Tauler, M. A. Cuevas-Diarte, and Y. Haget, *Powder Diffraction* **7,** 42 (1992).
10. H. Serrano-González, K. D. M. Harris, A. Álvarez-Larena, E. Estop, M. Labrador, and L. Palacios, manuscript in preparation.
11. C.-T. Ahn, S. Soled, and G. B. Carpenter, *Acta Crystallogr. B* **28,** 2152 (1972).
12. G. M. Sheldrick, SHELXL86, Program for the Solution of Crystal Structures, University of Göttingen, Germany, 1986.
13. G. M. Sheldrick, SHELXL93, Program for the Refinement of Crystal Structures, University of Göttingen, Germany, 1993.
14. J. Rodríguez-Carvajal, "1990 Abstracts of Satellite Meeting on Powder Diffraction of XVth Congress of the International Union of Crystallography (Toulouse, 1990)," p. 127.

15. J. C. van Miltenburg, A. Álvarez-Larena, M. Labrador, L. Palacios, J. Rodríguez-Romero, E. Tauler, and E. Estop, *Thermochimica Acta* **273,** 31 (1996).
16. J. Rodríguez-Romero, Treball de Fi de Carrera, Institut Químic de Sarrià (Barcelona), 1994.
17. F. H. Allen, O. Kennard, D. G. Watson, L. Brammer, A. G. Orpen, and R. Taylor, *J. Chem. Soc., Perkin Trans. II* S1 (1987).
18. V. Schomaker and K. N. Trueblood, *Acta Crystallogr. B* **24,** 63 (1968).
19. N. Ramasubbu, R. Parthasarathy, and P. Murray-Rust, *J. Am. Chem. Soc.* **108,** 4308 (1986).
20. X. Alcobé, E. Estop, A. E. Aliev, K. D. M. Harris, J. Rodríguez-Carvajal, and J. Rius, *J. Solid State Chem.* **110,** 20 (1994).
21. J. D. Gale, *J. Chem. Soc., Faraday Trans.* **93,** 629 (1997).
22. A. J. Pertsin and A. I. Kitaigorodsky, "The Atom-Atom Potential Method," Springer-Verlag, Berlin, 1987.